Applied Surface Science xxx (2014) xxx–xxx

Contents lists available at ScienceDirect

Applied Surface Science

journal homepage: www.elsevier.com/locate/apsusc

Structural, electrical and magnetic properties of epitaxial $La_{0.7}Sr_{0.3}CoO_3$ thin films grown on $SrTiO_3$ and $LaAlO_3$ substrates

Z. Othmen[a], A. Schulman[b,c,*], K. Daoudi[a,d], M. Boudard[b], C. Acha[c], H. Roussel[b], M. Oueslati[a], T. Tsuchiya[e]

[a] Unité Nanomatériaux et Photonique, Faculté des Sciences de Tunis, 2092 El Manar Tunis, Tunisia
[b] Laboratoire des Matériaux et du Génie Physique, UMR 5628 CNRS-UDG-Grenoble INP, Minatec 3, Parvis Louis Néel, CS 50257, 38016 Grenoble Cedex 1, France
[c] Departamento de Física, FCEyN, UBA and IFIBA, Conicet, Pabellón 1, Ciudad Universitaria, 1428 Buenos Aires, Argentina
[d] Physics Department, United Arab Emirates University, P.O. Box 17551, Al-Ain, United Arab Emirates
[e] National Institute of Advanced Industrial Science and Technology (AIST), Ibaraki 305-8565, Japan

ARTICLE INFO

Article history:
Received 2 November 2013
Received in revised form 26 February 2014
Accepted 5 March 2014
Available online xxx

Keywords:
Cobaltite thin films
Strain engineering
Conduction mechanism

ABSTRACT

$La_{0.7}Sr_{0.3}CoO_3$ (LSCO) thin films have been epitaxially grown on $SrTiO_3$ (STO) and $LaAlO_3$ (LAO) substrates by metal organic deposition. The effects of the strain – induced by clamping – on the structural and physical properties of the films were studied. For that, we have performed resistivity and magnetization studies as a function of temperature and magnetic field as well as X-ray diffraction and Raman spectroscopy measurements. Our X-ray results are similar for both substrates showing that the 20 nm films are fully strained while thicker films have two components corresponding to a fully strained and a relaxed component. Relaxation induced by increasing film thickness (up to 100 nm) results in a systematic evolution of the out of plane crystallographic cell parameter toward the bulk LSCO values. Raman spectra of the thinner films exhibit specific modes which are not present in the bulk LSCO spectra. These modes disappear for thicker films which are totally relaxed. All the samples show similar magnetic behavior independently of the thickness and the substrate with a Curie temperature (T_C) around 210 K. Relative changes in resistivity due to the film thickness are larger than 3 orders of magnitude with a relatively small influence of the type of strain induced by the substrate (compressive or tensile). Moreover whereas the relaxed film (100 nm thick) shows similar transport properties as the bulk sample, the fully strained film (20 nm thick) shows a 3D variable range hopping conduction with a higher degree of localization which is a direct result of the strain state.

1. Introduction

Hole-doped lanthanum cobaltite of general formula $La_{1-x}Sr_xCoO_3$ (LSCO) have created renewed research interest in the mixed valence transition metal-oxides with perovskite and related structures. Owing to their interesting magnetic and electrical properties, cobaltites in thin film form were increasingly requested in a wide range of applications, extending from component in solid oxides fuels cells, oxygen separation membranes and electrochemical reactors, to thermoelectric devices [1–3]. The physical properties of the LSCO material in bulk form are extremely sensitive to the chemical composition [4]. Moreover, when such material is prepared in thin film form, the physical properties are extremely sensitive to the growth method used, the deposition parameters and also the choice of the substrate which induce a strain that influence all the properties of the thin films. As have been reported previously, we expect substantial changes in the electrical conductivity and the magnetic properties of the films due to the strain which can be controlled by either changing the substrate material or the film thickness [5–11]. Understanding the mechanism responsible of these changes is particularly interesting, since it can be used to tune the film properties according to the requirements of the possible applications. LSCO films have already been epitaxially grown on several single crystalline substrates such as $LaAlO_3$ (LAO), $SrTiO_3$ (STO), $NdGaO_3$, $(LaAlO_3)_{0.3}–(SrAlTaO_6)_{0.7}$(LSAT), and $Pb(Mg_{1/3}Nb_{2/3})_{0.72}Ti_{0.28}O_3$

* Corresponding author at: Departamento de Física, FCEyN, UBA and IFIBA, Conicet, Pabellón 1, Ciudad Universitaria, 1428 Buenos Aires, Argentina.
Tel.: +54 1145763300276; fax: +54 1145763357.
E-mail address: schulman@df.uba.ar (A. Schulman).

http://dx.doi.org/10.1016/j.apsusc.2014.03.034
0169-4332/

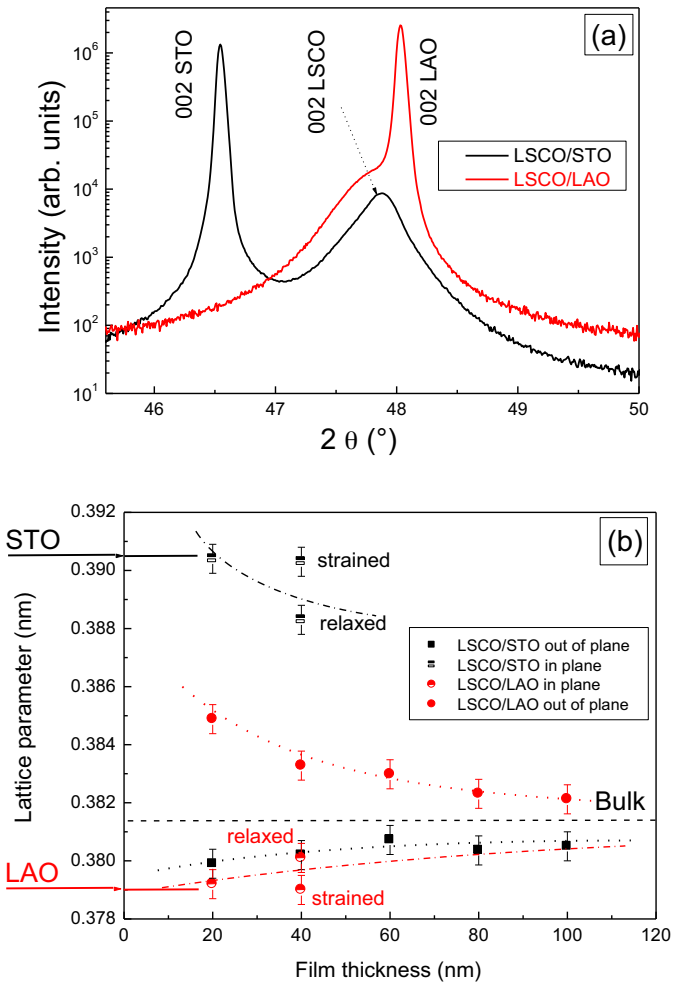

Fig. 1. (a) θ–2θ XRD scans around the 0 0 2 Bragg reflections of the 80 nm-thick LSCO films grown on LAO (red) and STO (black) substrates. (b) Lattice parameters vs. film thickness for LSCO grown on LAO and STO substrates using MOD process.

having relatively low lattice mismatches with the bulk LSCO material [5–11] but mostly by expensive techniques such as pulsed laser deposition or magnetron sputtering which usually requires high vacuum. Our previous works have demonstrated that epitaxial $La_{0.7}Sr_{0.3}CoO_3$ (LSCO) thin films can be successfully grown on STO substrates using a metal organic deposition (MOD) process which is a simpler and cheaper method [11]. In this paper, we report a study of the epitaxial growth and the corresponding structural and physical properties of the LSCO thin films on LAO and STO single-crystal substrates by MOD process. The effects of substrate material and the strain relaxation with film thickness are investigated using high resolution X-ray diffraction and Raman spectroscopy. Electrical and magnetic characteristics of the LSCO thin films were investigated and correlated to their corresponding structural properties.

2. Experimental

The LSCO thin films with thicknesses ranging from 20 nm to 100 nm were prepared by a conventional MOD process. The starting solution was prepared by mixing the constituent metal-naphthenate solution (Nihon Kagaku Sangyo) and diluting with toluene to obtain the required concentration and viscosity. The molar ratios of La, Sr and Co in the coating solution were 0.7, 0.3 and 1.0, respectively. This solution was spin-coated onto (0 0 1) single crystal STO and LAO substrates at 4000 rpm for 10 s. To eliminate the toluene, the metal-organic (MO) film was then dried in air at 100 °C for 10 min. Before the final annealing, a preheating step at 500 °C for 30 min is necessary to decompose the organic part. The preheating step is also required to prevent the formation of fissures on the film surface during the final thermal annealing at high temperature. To obtain a satisfactory film thickness, the above procedure (coating, drying, and preheating) was repeated several times (up to 5 times) giving rise to a corresponding number of superimposed layers in the LSCO product film. The final annealing was carried out in a conventional furnace at 1000 °C for 60 min in air. The film thicknesses have been precisely measured using transmission electron microscopy on cross-sections [11]. One deposited layer has a thickness around 20 nm. AFM and SEM measurements (not shown) reveal a smooth surface with a root mean square roughness of around 2 nm with no defects or cracks on the film surface with an homogeneous composition.

Phase purity and film crystallinity were examined by X-ray diffraction (XRD) in Bragg–Brentano geometry using a BRUKER D8 advance diffractometer with monochromatic CuKα1 radiation (λ = 0.154060 nm) and LynxEye 1 dimension detector. Reciprocal space mappings (RSM) were collected with a RIGAKU Smartlab equipped with a Cu rotating anode (9 kW). An incident high resolution setting was used (1D parabolic mirror and a two-crystal Ge monochromator in the 400 setting) leading to a monochromatic parallel X-ray beam (CuKα1). Optics used after the sample, were two 1.0 mm cross 10.0 mm slits, 2.5° sollers slits and a punctual scintillation counter detector.

Raman spectra were obtained at room temperature with a Horiba Jobin Yvon LabRam spectrometer using a 514.5 nm excitation wavelength.

Electrical transport measurements were performed using a four-terminal technique. Magnetic characterization was performed using a commercial SQUID magnetometer (Quantum Design, 5 T) with an applied magnetic field of 500 Oe in both the field cooled (FC) and zero field cooled (ZFC) measurements in the 5–400 K temperature range.

3. Results and discussions

3.1. Structural properties

3.1.1. XRD analysis

LSCO films have been systematically studied by XRD. These results show that the films have a single phase LSCO that have been epitaxially grown on top of the substrates. Typical θ–2θ XRD scans around the 0 0 2 Bragg reflections of the 80 nm-thick LSCO films grown on STO and LAO substrates are shown in Fig. 1(a). They show a (0 0 1) oriented LSCO films on both STO and LAO substrates. The 0 0 2 Bragg reflections of the LSCO films are nearly at the same positions for both substrates. Out-of-plane lattice parameters were obtained by θ–2θ scans for the whole thickness series whereas additional in plane values were obtained for 20 and 40 nm thick samples by RSM. Main results are summarized in Fig. 1(b) where pseudocubic values are used for representing the correlation between the in-plane and out of plane lattice parameters with the thickness of the films. For comparison cell parameter of the bulk LSCO (average pseudocubic values, 3.81 Å are derived from [12]), STO and LAO (average pseudocubic) are also represented. We can observe in Fig. 1(b) that increasing the film thickness from 20 to 60 nm is followed by an important change in the lattice parameters (in-plane and out-of-plane) for both substrates. The LAO and STO substrates impose different types of in-plane strains: the STO (a_{STO} = 3.905 Å) imposes a tensile strain while, in contrast, the LAO (a_{LAO} = 3.792 Å) imposes a compressive strain. We note that for both substrates the 20 nm thick LSCO films are fully strained with their

Please cite this article in press as: Z. Othmen, et al., Structural, electrical and magnetic properties of epitaxial $La_{0.7}Sr_{0.3}CoO_3$ thin films grown on $SrTiO_3$ and $LaAlO_3$ substrates, Appl. Surf. Sci. (2014), http://dx.doi.org/10.1016/j.apsusc.2014.03.034

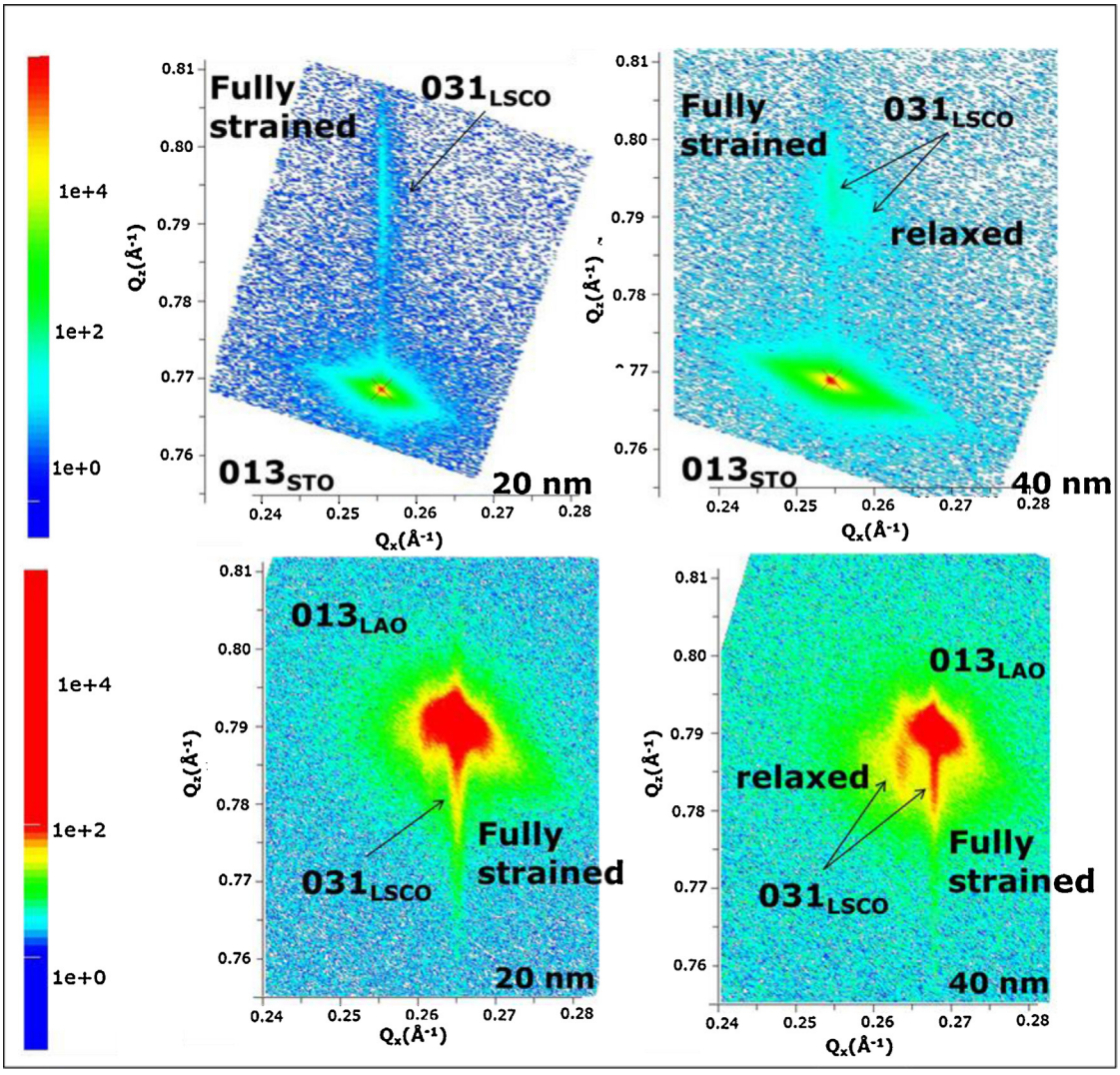

Fig. 2. Reciprocal space maps around the 0 1 3 Bragg reflection for the 20 and 40 nm thick LSCO films grown on LAO and STO substrates.

in-plane lattice parameters very close to those of the substrate materials and consequently very different than that of the bulk material. By increasing the film thickness to 40 nm or higher we note a strain relaxation evidenced by an important decrease of the in-plane lattice parameter of the LSCO film in the case of STO substrate and an increase in the case of the LAO substrate. For thicker films the values of the crystallographic out-of-plane cell parameter become closer to that of the bulk material.

In this study, the strain is varied by varying the substrate material and the film thickness. A drastic effect of the varied strain is observed in the reciprocal space map (RSM) around the 0 1 3 reflection for the films having 20 and 40 nm in thickness grown on STO and LAO substrates (Fig. 2). Due to the relatively large lattice mismatch (δ_{STO} = 2.33%) between LSCO and STO, the 0 1 3 reflections for the film and the substrate are easily distinguished in comparison to the reflections of the LSCO film and LAO substrate (δ_{LAO} = −0.58%). Looking at the 20 nm film grown on STO, we observe a symmetric lobe of intensity at the STO 0 1 3 reflection and a streak of intensity from the LSCO film 0 1 3. In the case of the 20 nm film grown on LAO, the 0 1 3 reflection of the LSCO film appears also in the shape of a streak of intensity and is found in this case to be superimposed on that of the LAO substrate. For both substrates the streak is aligned along the Q_z direction, indicating that the broadening in Q_z is much more important than that in $Q_{x,y}$. This broadening in Q_z occurs due to the usual finite-size effects for such thin films, while the narrow shape in $Q_{x,y}$ indicates high in-plane correlation lengths with almost no mosaic spread. Such effect of broadening in the Q_z has been evidenced for thinner film in the θ–2θ XRD patterns of the LSCO grown on STO substrates [11]. Increasing the film thickness to 40 nm results – as expected – in a narrower distribution along the Q_z direction. Interestingly, a wider distribution along $Q_{x,y}$ with respect to the 20 nm film is observed, this corresponds to a multi component contribution for both LAO and STO substrates with two different origins: while one is due to the fully strained film close to the substrate as the one observed for the 20 nm film, the second component originates from a relaxed film corresponding to the top part of the sample. The detailed evolutions of the in plane and out of plane lattice parameters of both components are shown in Fig. 1. Whereas the fully strained component is easily identified in Figs. 1 and 2 as its in-plane parameter is the same as the substrate, the cell parameters of the relaxed component evolve toward the bulk values. We can conclude that thinner films (20 nm) are fully strained and that the strain relaxation process occurs at higher thickness.

3.1.2. Raman spectroscopy measurements

Raman spectroscopy was used as a complementary study of the XRD due to its sensitivity to small changes in symmetry and to

Please cite this article in press as: Z. Othmen, et al., Structural, electrical and magnetic properties of epitaxial $La_{0.7}Sr_{0.3}CoO_3$ thin films grown on $SrTiO_3$ and $LaAlO_3$ substrates, Appl. Surf. Sci. (2014), http://dx.doi.org/10.1016/j.apsusc.2014.03.034

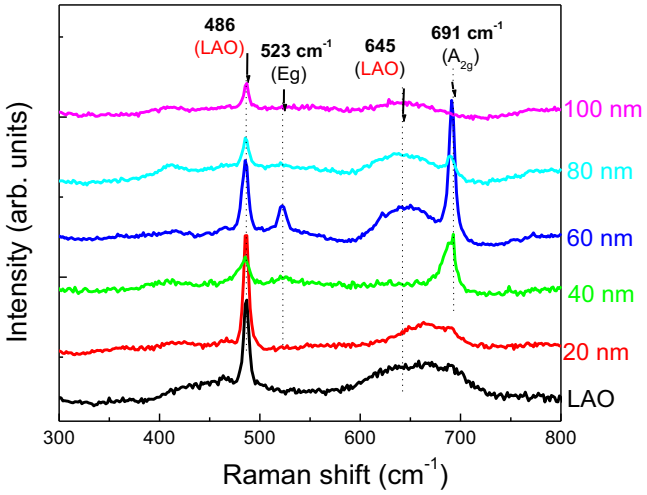

Fig. 3. Room-temperature Raman spectra vs. thickness of the LSCO films grown on LAO substrates using MOD process.

applied stress. The Raman modes of the LSCO films and of the STO substrates were found to overlap (not shown here) precluding any further analysis. On the other hand, the LSCO thin films grown on the LAO substrates show interesting evolution in the Raman spectra with respect to the film thickness (Fig. 3). The Raman spectrum of the LAO substrate is shown as a reference. The Raman spectrum of the LAO substrate is mainly dominated by a sharp peak centered around 486 cm^{-1} and a large peak around 645 cm^{-1}. In the rhombohedrally distorted perovskite structure of the $R\bar{3}c$ symmetry, Raman active modes are $A_{1g} + 4E_g$ and the infrared actives modes are $3A_{2u} + 5E_u$ [13,14]. The main two peaks of the LAO Raman spectrum (Fig. 3) have been assigned to E_g mode at 486 cm^{-1} (pure oxygen bending vibration), and E_g mode at 645 cm^{-1} (out-of phase stretching oxygen vibration), respectively [13]. The Raman spectrum of the 20 nm thick LSCO film on LAO is found to be similar to the spectrum of the LAO substrate. The contribution of the relatively thin film (20 nm) to the Raman spectrum of the LSCO/LAO system is minimal and do not appear in the spectrum. On the other hand, by increasing the film thickness to 40 nm, in addition to the characteristic modes of the LAO substrate we note the appearance of a Raman mode at 691 cm^{-1}. Furthermore, for the 60 nm thick film we note an important increase of the intensity of 691 cm^{-1} peak and the appearance of a second Raman mode centered at 523 cm^{-1}. The 523 cm^{-1} and 691 cm^{-1} modes are assigned to the E_g quadruple mode and to the breathing A_{2g} mode, respectively [15,16]. By increasing the film thickness to 80 nm we note an important decrease of the intensities of these two peaks that finally disappear for a thickness of 100 nm. The 100 nm thick LSCO films should be fully relaxed with similar vibrational properties than the bulk material [15,16] whereas strain in the thinner films is characterized by the 523 and 691 cm^{-1} modes. As far as this last mode is considered we note that similar results have been reported on $La_{0.67}Ca_{0.33}MnO_3$ (LCMO) films grown on LAO – exhibiting an intense mode around 690 cm^{-1} which is not observed in bulk sample [17] – and on the undoped compound $LaCoO_3$ [16].

3.2. Electrical transport properties

The effect of the strain is further evidenced in the electrical transport properties of the LSCO films. In Fig. 4(a) we show the temperature dependence of the resistivity for the LSCO films with two different thicknesses (20 and 100 nm) grown on LAO and STO substrates. Regardless the type of the substrate material, the film resistivity was found to be considerable decreased by several orders

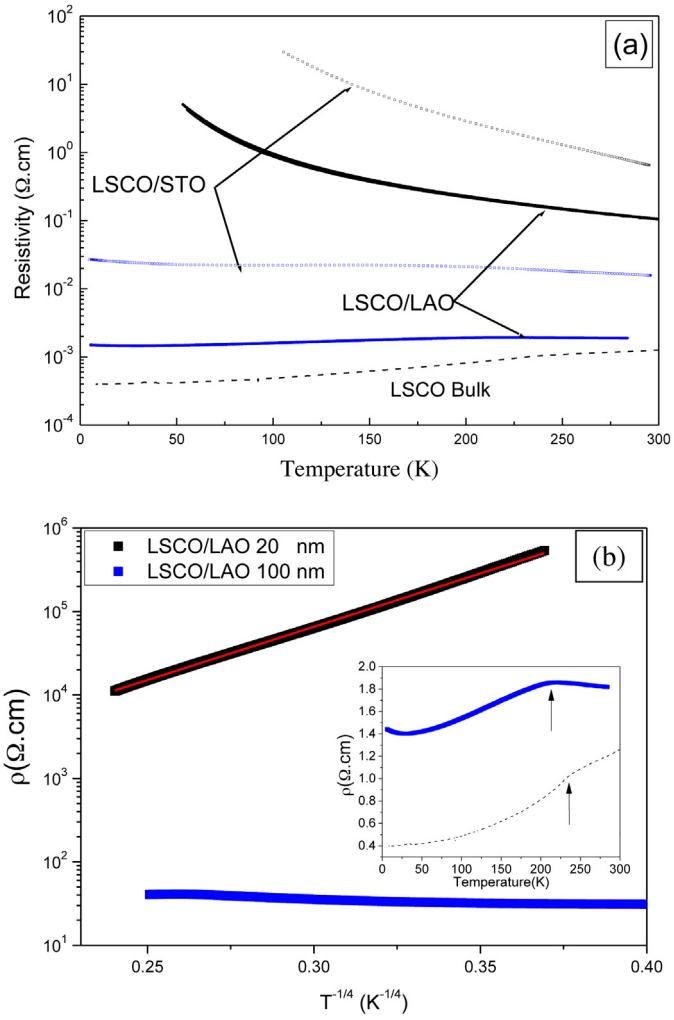

Fig. 4. (a) Temperature dependence of resistivity of the 20 nm (black symbols) and 100 nm (blue symbols) thick LSCO films grown on LAO and STO substrates. Data corresponding to a bulk sample (dashed line) are provided for comparison. (b) $\rho(T)$ versus $T^{-1/4}$ for the 20 nm and 100 nm films grown on LAO substrate. The inset shows the metallic behavior of the thicker film grown on LAO (blue symbols) along with the bulk sample (dashed line). The arrows indicate the magnetic transition temperatures T_C (see text).

of magnitude by increasing the film thickness to 100 nm. We also observe a smooth transition from the insulating thinner films to the metallic thicker ones in function of film thickness (not shown), where not only the value of the room temperature resistivity is changed but also their conduction mechanism. We have enough evidence to believe that the changes observed in the electrical transport properties are originated essentially by the strain induced by the substrate and are not an effect of size or any external factor (e.g. micro-cracks or grain boundary conduction). Further indication of this scenario arises when noting that LSCO films grown on LAO substrates – imposing relatively low strain state – are always more conductive than those grown on STO substrates – imposing relatively large strain.

For the 20 nm thick LSCO films grown on both substrates, $\log(\rho)$ was found to be proportional to $(T/T_0)^{-1/4}$ (Fig. 4(b) only 20 nm film on LAO is shown) which is a clear indication that the conduction mechanism is dominated by a 3D variable range hopping (VRH) – in agreement to previous works [9] – which entails the localization of the charge carriers in a disordered system. In the VRH model [18], T_0 depends on the electron localization length l, and the density of states at the Fermi level $N(E_f)$: $k_b T_0 = 18/[l^3 N(E_f)]$ where k_b is

Please cite this article in press as: Z. Othmen, et al., Structural, electrical and magnetic properties of epitaxial $La_{0.7}Sr_{0.3}CoO_3$ thin films grown on $SrTiO_3$ and $LaAlO_3$ substrates, Appl. Surf. Sci. (2014), http://dx.doi.org/10.1016/j.apsusc.2014.03.034

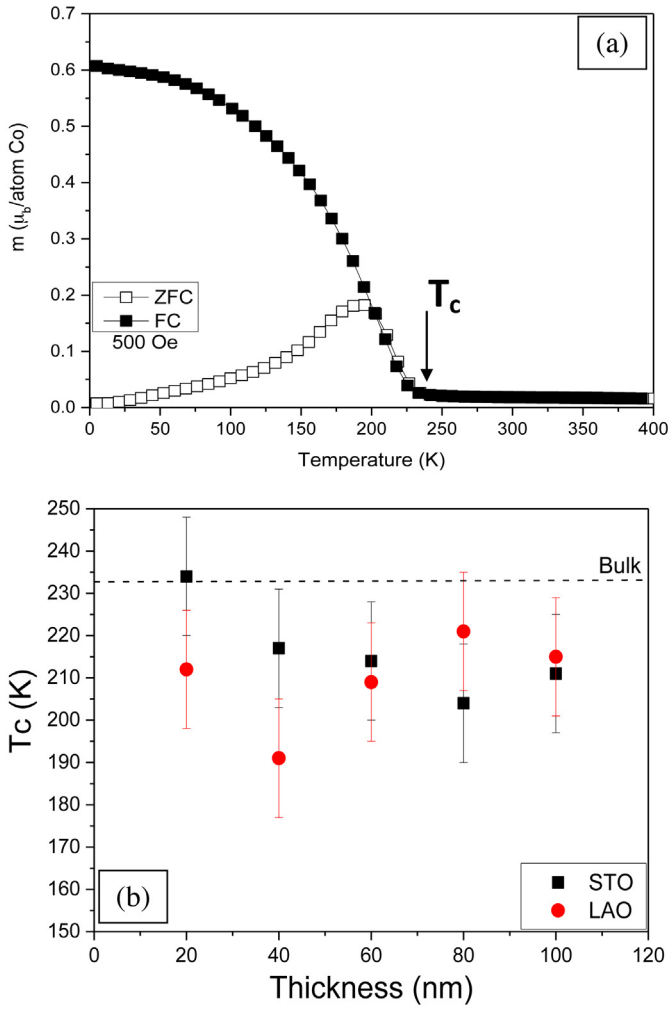

Fig. 5. (a) Temperature dependence of the magnetization of the 60 nm thick LSCO film grown on STO substrate. (b) Evolution of the T_C versus films thickness for LAO and STO substrates. T_C were deduced by linear extrapolation of the square magnetization to zero ($M^2(T_C)=0$). T_C corresponding to a bulk sample (dashed line) is provided for comparison.

the Boltzmann constant. Using the e_g bandwidth, $\Delta e_g \approx 0.3$ eV [19] and the carrier concentration n induced by the Sr doping together with the $T_0 = 1.24 \times 10^5$ K (resp. $T_0 = 2.26 \times 10^5$ K) obtained from the resistivity measurements for the 20 nm thick samples grown on LAO (resp. STO) substrate, we estimate the localization length $l = 0.5$ nm (LAO) and $l = 0.41$ nm (STO) which are comparable with the results of Fuchs et al. obtained in LSAT substrate [9].

However, for the 100 nm thick LSCO film the VRH conduction mechanism model is not appropriate (a positive slope as the one observed for the 20 nm film in Fig. 4b is required for validation of this model). The 100 nm thick LSCO film displays metallic conductivity at all temperatures similarly to the bulk LSCO compound (inset of Fig. 4b) where the conduction behavior is dominated by the double exchange mechanism which is typical for complex oxides with perovskite crystal structures [20]. As seen in the inset of Fig. 4b, both the bulk and thicker films show a kink in the resistivity near the Curie temperature (T_C) as expected for a perovskite system dominated by double exchange mechanism where the magnetism and the transport properties are coupled. The effect of the magnetism in the conduction becomes negligible as the films become thinner and the effect of the strain becomes more important inducing the disorder necessary to change the conduction mechanism to the VRH which is less affected by the magnetism of the sample.

3.3. Magnetic properties

With respect to the magnetic behavior, all samples show similar characteristics to the bulk [20,21] regardless of the thicknesses and the substrate. A typical M(T) curve of the 60 nm thick LSCO film grown on STO substrate is shown in Fig. 5(a) as an example. The FC M(T) shows a ferromagnetic-like transition and T_C is marked in Fig. 5(a). Below T_C, the film exhibits a ferromagnetic-like behavior and above it is in a paramagnetic state. Almost no change in T_C was observed as a function of the thickness or the substrate (Fig. 5(b)) and our results are in good agreement with those of Rata et al. [6]. The present work shows that the magnetic behavior is similar for all types of samples with a relatively small influence of the type of stress induced by the substrate (compressive or tensile).

Though the sample present dominant ferromagnetic interactions the exact nature of the magnetic order is certainly more complicated and is beyond the scope of the present work. Indeed the magnetization curves shows the typical λ shape characteristic of spin glass systems resulting from competing magnetic interactions which coexist on both sides of the magnetic transition with different magnetic orders like FM and paramagnetic domains which are also observed in bulk samples [21,22].

4. Conclusion

Epitaxial LSCO films have been epitaxially grown on single crystalline substrates of LAO and STO. The effects of epitaxial strain and film thickness on the lattice structure, electrical conduction and magnetization have been studied using thickness-dependent series on lattice-mismatching single-crystalline substrates. The 20 nm thick films were found fully strained for both substrates while the higher thicknesses show partial relaxation characterized by the appearance of a relaxed component in the film that presents an evolution of in-plane and out-of-plane lattice parameter toward the bulk value. The evolution of the Raman spectra with film thickness is directly correlated to the strain relaxation. All samples show a similar magnetic behavior to the bulk material, regardless of the substrate and the thickness indicating that the strain is not an important factor in magnetism for these types of samples. The resistivity of the samples is lowered almost three orders of magnitude when the thickness is changed from 20 nm to 100 nm for both substrates which is a direct result of the strain state induced by the substrates with a relatively small influence of the type of strain induced (compressive or tensile).

Acknowledgements

AS acknowledges scholarships from the European Commission (Arcoiris Erasmus Mundus), the University of Buenos Aires and from CONICET (Argentina). We are grateful with O. Chaix-Pluchery (Raman spectroscopy) and with F. Gay (resistivity measurements) for their experimental assistance.

References

[1] J. Mizusaki, J. Tabuchi, T. Matsuura, S. Yamauchi, K. Fueki, J. Electrochem. Soc. 136 (1989) 2082.
[2] Y. Ohno, S. Nagata, H. Sato, Solid State Ion. 9 (1983) 1001.
[3] A. Maignan, S. Hebert, L. Pi, D. Pelloquin, C. Martin, C. Michel, M. Hervieu, B. Raveau, Crystal Eng. 5 (2002) 365.
[4] H.M. Aarbogh, J. Wu, L. Wang, H. Zheng, J.F. Mitchell, C. Leighton, Phys. Rev. B 74 (2006) 134408.
[5] M.A. Torija, M. Sharma, M.R. Fitzsimmons, M. Varela, C. Leighton, J. Appl. Phys. 104 (2008) 023901.
[6] A.D. Rata, A. Herklotz, K. Nenkov, L. Schultz, K. Dorr, Phys. Rev. Lett. 100 (2008) 076401.
[7] L. Malavasi, E. Quartarone, C. Sanna, N. Lampis, A.G. Lehmann, C. Tealdi, M.C. Mozzati, G. Flor, Chem. Mater. 18 (2006) 5230.
[8] D. Fuchs, O. Moran, P. Adelmann, R. Schneider, Physica B 349 (2004) 337.

Please cite this article in press as: Z. Othmen, et al., Structural, electrical and magnetic properties of epitaxial $La_{0.7}Sr_{0.3}CoO_3$ thin films grown on $SrTiO_3$ and $LaAlO_3$ substrates, Appl. Surf. Sci. (2014), http://dx.doi.org/10.1016/j.apsusc.2014.03.034

[9] D. Fuchs, T. Schwarz, O. Moran, P. Schweiss, R. Schneider, Phys. Rev. B 71 (2005) 092406.
[10] J.R. Sun, H.W. Yeung, H. Li, K. Zhao, H.N. Chan, H.K. Wong, J. Appl. Phys. 90 (2001) 2831.
[11] K. Daoudi, T. Tsuchiya, T. Nakajima, A. Fouzri, M. Oueslati, J. Alloys Compd. 506 (2010) 483.
[12] R. Caciuffo, D. Rinaldi, G. Barucca, J. Mira, J. Rivas, M.A. Senaris-Rodriguez, P.G. Radaelli, D. Fiorani, J.B. Goodenough, Phys. Rev. B 59 (1999) 1068.
[13] M.V. Abrashev, A.P. Litvinchuk, M.N. Iliev, R.L. Meng, V.N. Popov, V.G. Ivanov, R.A. Chakalov, C. Thomsen, Phys. Rev. B 59 (1999) 4146.
[14] J. Suda, O. Kamishima, J. Kawamura, T. Hattori, T. Sato, J. Phys: Conf. Ser. 150 (2009) 052249.
[15] A. Ishikawa, J. Nohara, S. Sugai, Phys. Rev. Lett. 93 (2004) 136401.
[16] N. Orlovskaya, D. Stenmetz, S. Yarmolenko, D. Pai, J. Sankar, J. Goodenough, Phys. Rev. B 72 (2005) 014122.
[17] Y.M. Xiong, T. Chen, G.Y. Wang, X.H. Chen, X. Chen, C.L. Chen, Phys. Rev. B 70 (2004) 094407.
[18] N.F. Mott, Metal-Insulator Transitions, 2nd ed., Taylor and Francis, London, 1990.
[19] M. Imada, A. Fujimori, Y. Tokura, Rev. Mod. Phys. 70 (1998) 1039.
[20] M. Kriener, C. Zobel, A. Reichl, J. Baier, M. Cwik, K. Berggold, H. Kierspel, O. Zabara, A. Freimuth, T. Lorenz, Phys. Rev. B 69 (2004) 094417.
[21] M. Itoh, I. Natori, S. Kubota, K. Motoya, J. Phys. Soc. Jpn. 63 (1994) 1486.
[22] P.L. Kuhns, M.J.R. Hoch, W.G. Moulton, A.P. Reyes, J. Wu, C. Leighton, Phys. Rev. Lett. 91 (2003) 127202.

Please cite this article in press as: Z. Othmen, et al., Structural, electrical and magnetic properties of epitaxial $La_{0.7}Sr_{0.3}CoO_3$ thin films grown on $SrTiO_3$ and $LaAlO_3$ substrates, Appl. Surf. Sci. (2014), http://dx.doi.org/10.1016/j.apsusc.2014.03.034